

# A Review of Neutrino Physics: Masses and Flavor Changing

James Hirschauer

*University of Colorado at Boulder, Boulder, CO 80309-0390*

(Dated: May 17, 2005)

## Abstract

Mixing between neutrino flavors has been indicated to varying degree in studies of solar, atmospheric, reactor, and now accelerator neutrinos. Mixing implies the existence of a mass basis related to the weak basis by a unitary transformation (MNS) matrix and non-zero mass for at least one mass eigenstate. The standard parametrization of vacuum transition probabilities for quasi-two-neutrino and one mass-scale, three-neutrino mixing are derived and related to the parameterization of the MNS matrix. The Mikheyev-Smirnov-Wolfenstein theory of neutrino propagation through solar matter is also described. The characteristic  $\Delta m^2$ - $\sin^2 2\theta$  parameter space and the methods for determining its favored and excluded regions are described.

The results of six important experiments from diverse sectors are presented and related to one another. Current best-fit values and limits for the  $\Delta m^2$ - $\sin^2 2\theta$  parameters are shown within the context of a sensible chronology. The LSND measurement is shown to conflict with current theory, implying the existence of sterile neutrinos. The future long-baseline, high-energy accelerator oscillation searches are also briefly described. The intrinsic nature of neutrino mass, Majorana or Dirac, while not included in this review, will be addressed in the accompanying presentation.

## Contents

<b>1. Historical Introduction</b>	2
<b>2. Mixing and Mass as Mutual Consequences</b>	3
2.1. Mixing in Vacuum	4
<b>3. Experimental Implications</b>	5
3.1. Accessible Region of Parameter Space	6
<b>4. Simplifying Assumptions</b>	8
4.1. Three Neutrino Mixing	8
<b>5. The Solar Neutrino Problem</b>	10
5.1. Super-Kamiokande and SNO	10
5.2. Theory of Solar Neutrino Oscillation: Matter Matters	11
5.3. KamLAND	12
<b>6. The Atmospheric Neutrino Problem</b>	13
6.1. Super-Kamiokande - Atmospheric Mode	14
6.2. The CHOOZ Experiment	15
<b>7. Constraining the Parameters - Summary</b>	16
<b>8. Outstanding Issues: The LSND Problem</b>	16
<b>9. Conclusion and Future Experiments</b>	18
<b>References</b>	19

## 1. HISTORICAL INTRODUCTION

In 1914, J. Chadwick observed the continuous energy spectrum of electrons emitted during nuclear beta decay to differ from the discrete spectra of alpha and gamma decay. Experiments using the  $\beta$ -decay of  $^{210}\text{Bi}$  nuclei by C.D. Ellis and L. Meitner confirmed Ellis's theory that the spectrum is that of electrons from the primary  $\beta$ -decay and precluded Meitner's

theory that the electrons are from secondary processes that broaden the initially discrete spectrum. To explain this peculiarity, N. Bohr speculated that conservation of energy holds only statistically in the interaction underlying  $\beta$ -decay. W. Pauli found this idea distasteful, and, at a conference in Pasadena in 1931, proposed, “The conservation laws remain valid, since the emission of the  $\beta$ -particles is accompanied by a very penetrating radiation of neutral particles, which has not been observed up to now [1].”

The neutrino, or more precisely, the anti-neutrino was first observed by C.L. Cowan and F. Reines in 1956 through inverse  $\beta$ -decay,  $\bar{\nu}_e + p \rightarrow e^+ + n$ , in a mixture of water and cadmium chloride [2]. Cowan and Reines detected the delayed coincidence of the annihilation photons of the positron and the photons emitted during the capture of the neutron by a  $^{113}\text{Cd}$  nucleus 10  $\mu\text{s}$  later. In 1955 at the Brookhaven reactor, R. Davis found evidence consistent with the fact that the neutrino and anti-neutrino are different particles. Obvious proof that  $\nu = \bar{\nu}$  would be observation of the process  $\nu_e + p \rightarrow e^+ + n$ . Lacking a  $\nu_e$  source, Davis instead looked for the inverse process  $\bar{\nu}_e + n \rightarrow e^- + p$  in the reaction  $\bar{\nu}_e + {}^{37}\text{Cl} \rightarrow e^- + {}^{37}\text{Ar}$ , observed no signal, and set a lower limit on the reaction cross section [3]. At the Brookhaven AGS in 1959, B. Pontecorvo showed that  $\nu_e \neq \nu_\mu$  by observing that those  $\nu_\mu$  created during the decay of charged pions did not produce electrons in subsequent interactions with nuclei in the detector.

More recently, in 2001 the four experiments at LEP combined results and fit the decay width of the  $Z^0$  boson for different numbers of light ( $m_\nu < m_Z/2$ ) neutrino flavors. The best-fit value  $N_f = 2.984 \pm 0.008$  [4] is clearly consistent with the expectation of three flavors. However, this measurement only restricts the number of light neutrinos that couple with the  $Z^0$ .

## 2. MIXING AND MASS AS MUTUAL CONSEQUENCES

The earliest  $\beta$ -decay spectra were consistent with a neutrino mass of zero, and the mass was taken to be identically zero in the Standard Model. Recent *direct* mass searches using the  $\beta$ -decay of tritium ( ${}^3\text{H} \rightarrow {}^3\text{He}^+ + e^- + \bar{\nu}_e$ ) place upper limits (95% C.L.) on the mass of the  $\nu_e$  averaging to 3 eV [4].

While ineffective for measuring absolute mass, the observation of neutrino flavor mixing necessitates a non-zero mass for at least one mass eigenstate. There is compelling evi-

dence from the solar and atmospheric neutrino sectors that neutrinos change flavor, see Secs. (6.1 & 5.2). The simplest explanation for this phenomenon is the existence of two different neutrino bases, namely, the weak and mass bases.

## 2.1. Mixing in Vacuum

To be general, one assumes  $n$  number of orthonormal weak (flavor) eigenstates called  $|\nu_f\rangle$  for  $f = \{e, \mu, \tau, \dots\}$  and  $n$  mass eigenstates called  $|\nu_i\rangle$  for  $i = \{1, 2, 3, \dots\}$ . Just as in the quark sector with the CKM matrix, these bases are related by a unitary matrix  $U_{fi}$  as

$$|\nu_f\rangle = \sum_{i=1}^n U_{fi} |\nu_i\rangle \quad \text{and} \quad |\nu_i\rangle = \sum_{f=1}^n U_{if}^* |\nu_f\rangle. \quad (1)$$

Neutrinos are created in weak interactions as  $|\nu_f\rangle$ , and since they only participate in the weak interaction can time-evolve “without interruption.” In the quark sector, there is no oscillation because quarks resulting from weak processes are immediately forced into a stationary state by the ubiquitous strong interaction. To quantify the time-evolution of relativistic neutrinos in vacuum, notice that the mass eigenstates have the typical space and time dependence of a free particle [5]

$$|\nu_i(x, t)\rangle = e^{-\frac{i}{\hbar}(E_i t - p_i x)} |\nu_i(x, t=0)\rangle \quad (2)$$

where  $t$  and  $x$  are measured in the laboratory.

The ultra-relativistic neutrino travels a distance  $L$  in time  $t$  such that  $L = ct$ ; and its mass, energy, and momentum are related by  $E \approx p \gg m$ . Assuming that each mass component of  $|\nu_f\rangle$  has the same momentum  $p$  and Taylor expanding in  $m_i^2/p^2$ , one can write

$$E_i = (p^2 + m_i^2)^{\frac{1}{2}} = p \left(1 + \frac{m_i^2}{p^2}\right)^{\frac{1}{2}} \approx p + \frac{m_i^2}{2p}. \quad (3)$$

Setting  $\hbar = c = 1$ , one can rewrite Eq. (2)

$$|\nu_i(x, t)\rangle = e^{-i(p + \frac{m_i^2}{2p})t - ipx} |\nu_i\rangle \quad (4)$$

$$|\nu_i(x = t = L)\rangle = e^{-i\frac{m_i^2}{2} \frac{L}{p}} |\nu_i\rangle = e^{-i\frac{m_i^2}{2} \frac{L}{E}} |\nu_i\rangle, \quad (5)$$

and inserting this expression for a time-evolving mass eigenstate into Eq. (1), one finds

$$|\nu_f(t)\rangle = |\nu(L)\rangle = \sum_{i=1}^n U_{fi} e^{-i\frac{m_i^2}{2} \frac{L}{E}} |\nu_i\rangle. \quad (6)$$

The time dependent amplitude for a transition  $|\nu_f\rangle \rightarrow |\nu_{f'}\rangle$ , measured at a distance  $x = L$  from the birth of  $|\nu_f\rangle$ , is  $\langle \nu_{f'} | \nu(L) \rangle$ . Using the complement of Eq. (1) to express  $\langle \nu_{f'} |$  in the mass basis, one can write the transition amplitude as

$$\langle \nu_{f'} | \nu(L) \rangle = \sum_i U_{f'i}^* U_{fi} e^{-i \frac{m_i^2}{2} \frac{L}{E}}. \quad (7)$$

The vacuum transition probability, with  $\Delta m_{ij}^2 \equiv m_i^2 - m_j^2$  and  $K_{ff'ij} \equiv U_{fi} U_{f'j}^* U_{f'j} U_{fi}^*$ , can be written

$$|\langle \nu_{f'} | \nu(L) \rangle|^2 = \sum_{i=j} U_{fi} U_{f'j}^* U_{f'j} U_{fi}^* + \sum_{i \neq j} K_{ff'ij} e^{-i \frac{\Delta m_{ij}^2}{2} \frac{L}{E}} \quad (8)$$

$$= \sum_i |U_{fi} U_{f'i}^*|^2 + \sum_{i>j} K_{ff'ij} e^{-i \frac{\Delta m_{ij}^2}{2} \frac{L}{E}} + K_{ff'ji} e^{i \frac{\Delta m_{ij}^2}{2} \frac{L}{E}} \quad (9)$$

$$= \left| \sum_i U_{fi} U_{f'i}^* \right|^2 + \sum_{i>j} K_{ff'ij} (e^{-i \frac{\Delta m_{ij}^2}{2} \frac{L}{E}} - 1) + K_{ff'ji} (e^{i \frac{\Delta m_{ij}^2}{2} \frac{L}{E}} - 1). \quad (10)$$

Noting that  $K_{ff'ij} = K_{ff'ji}^*$  and that the unitarity of  $U$  ensures

$$\sum_i U_{fi} U_{f'i}^* = \delta_{ff'}, \quad (11)$$

one can write the probability as

$$\begin{aligned} |\langle \nu_{f'} | \nu(L) \rangle|^2 &= \delta_{ff'} - 4 \sum_{i>j} \text{Re}(K_{ff'ij}) \sin^2\left(\frac{\Delta m_{ij}^2}{4} \frac{L}{E}\right) \\ &\quad + 4 \sum_{i>j} \text{Im}(K_{ff'ij}) \sin\left(\frac{\Delta m_{ij}^2}{4} \frac{L}{E}\right) \cos\left(\frac{\Delta m_{ij}^2}{4} \frac{L}{E}\right). \end{aligned} \quad (12)$$

There will be no mixing unless at least one off-diagonal element is non-zero *and* one stationary state has a mass different from any of the others,  $\Delta m_{ij}^2 \neq 0$ . In this way the observation of neutrino oscillations proves that  $m_{\nu_i} > 0$  for at least one mass state  $i$ .

### 3. EXPERIMENTAL IMPLICATIONS

The form of Eq. (12) influences the design of experimental searches for neutrino oscillation. A primary concern are the flavors  $f$  and  $f'$ . The initial flavor  $f$  is determined by the choice of source of which there are essentially four: the Sun (supplying  $\nu_e$ ), cosmic rays interacting with the atmosphere ( $\nu_e, \nu_\mu, \bar{\nu}_e, \bar{\nu}_\mu$ ), nuclear reactors ( $\bar{\nu}_e$ ), and particle accelerators ( $\nu_e, \nu_\mu, \bar{\nu}_e, \bar{\nu}_\mu$ ). Being created only with the heavy  $\tau$  lepton, the  $\nu_\tau$  is rare and not exploited

experimentally as an initial state. Choices of final flavor  $f'$  ramify oscillation searches into two types: *appearance* and *disappearance* experiments. For instance, one can search for an excess of  $\nu_e$  coming from an accelerator beam of mostly  $\nu_\mu$ , or one can search for a deficit in the expected number of  $\nu_e$  coming from the sun. Additionally, neutrinos of different flavors  $f'$  require different methods of detection.

With some restriction, the quantity  $L/E$  is decided by the experimentalist in accelerator and reactor experiments. In accelerator experiments where  $E$  can be tuned, the energy of the detected charged-particle must be greater than detector threshold. In reactor experiments,  $L$  is limited because neutrino flux falls off as  $1/L^2$ . Clearly, in solar neutrino studies, the value  $L/E$  is not at all determined by scientists, but is believed to be known theoretically. The energy of atmospheric neutrinos is also uncontrolled, but atmospheric neutrino studies are afforded two baselines differing by three orders of magnitudes: one from above through 10 km of atmosphere and one from below through 12,000 km of earth.

### 3.1. Accessible Region of Parameter Space

The most important consequences of Eq. (12) are the definition of the parameter space to be investigated and the determination of the region of that space accessible to a given experiment. The theoretical transition probability is characterized by a two-dimensional parameter space: the difference of the squares of the masses (the *mass-splitting*)  $\Delta m_{ij}^2$  versus the product of matrix elements  $K_{ff'ij}$ .

The accessible range of  $\Delta m_{ij}^2$  is determined by the relationship of the experiment parameter  $L/E$  to the mass-splitting:  $\Delta m_{ij}^2 L/4E$ . For maximum sensitivity to oscillation, this quantity must be on the order of unity and so  $L/4E \sim 1/\Delta m_{ij}^2$ . As seen in Fig. (1), when  $L/4E \ll 1/\Delta m_{ij}^2$ , oscillation is minimal because the measurement is made before the oscillations have begun to appreciably develop. When  $L/4E \gg 1/\Delta m_{ij}^2$ , detector resolution allows only an average transition probability to be measured.

In practice, sources provide a spectrum of neutrino energies, and it is hoped that this spectrum can be used to make measurements of the oscillation pattern in the blue-framed regions in Fig. (1), as done in Fig. (3). In this sensitive region, oscillation has begun *and* steps through the spectrum of neutrino energy ( $E$ ) on the order of detector resolution result in gradual changes in transition probability. Table (I) shows the  $\Delta m^2$  sensitivity for

experiments with different values of  $L$  and  $E$ . In addition to observing oscillation signature,

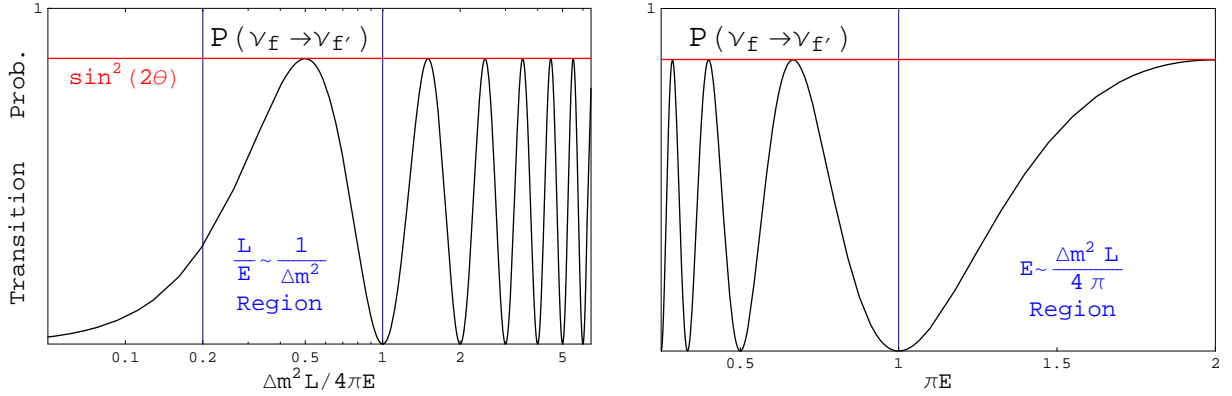


FIG. 1: Logarithmic plot of the transition probability for oscillation  $\nu_f \rightarrow \nu_{f'}$  versus  $\Delta m^2 L/4E$  (left). Plot of transition probability with fixed  $\Delta m^2 L$  versus  $\pi E$  (right); large  $L/E \rightarrow$  small  $E$  where even small  $\Delta E$  results in large change in  $P(\nu_f \rightarrow \nu_{f'})$ . The regions of maximum sensitivity are bordered above and below in blue. The maximum probability (red) is characterized by  $K_{ff'ij}$  which looking ahead has been written  $\sin^2(2\theta)$ .

experiments hope to measure the parameters characterizing lepton mixing, but to do this Eq. (12) must be simplified.

Experiment Type	$\nu_f$ Energy (MeV)	Distance (m)	$\Delta m^2$ Sensitivity	Represent. Experiment
Solar Neutrinos	10	$10^{11}$	$10^{-10}$ eV <sup>2</sup>	SNO
Atmospheric Neutrinos	$10^3$	$10^7$	$10^{-4}$ eV <sup>2</sup>	SuperK
Reactor (LBL)	10	$10^5$	$10^{-4}$ eV <sup>2</sup>	KamLAND
High $E$ Accel. (LBL)	$10^3$	$10^6$	$10^{-3}$ eV <sup>2</sup>	MINOS
Reactor (SBL)	10	$10^3$	$10^{-2}$ eV <sup>2</sup>	CHOOZ
High $E$ Accel. (SBL)	$10^3$	$10^3$	1 eV <sup>2</sup>	MiniBooNE

TABLE I: Nominal sensitivity to  $\Delta m^2$  for six experiments with various  $L/E$  values. A spectrum of  $\nu_f$  energy allows for sensitivity to a couple orders of magnitude in  $\Delta m^2$ . “LBL” means “long base line” and “SBL” means “short base line.”

## 4. SIMPLIFYING ASSUMPTIONS

Under certain circumstances, Eq. (12) can be simplified significantly by adopting the assumption of “quasi-two-neutrino oscillation [4].” In this regime, the initial and final flavor states couple strongly to only two mass eigenstates so that the unitary relation can be parametrized by one real angle as

$$\begin{pmatrix} \nu_f \\ \nu_{f'} \end{pmatrix} = \begin{pmatrix} \cos \theta & \sin \theta \\ -\sin \theta & \cos \theta \end{pmatrix} \begin{pmatrix} \nu_1 \\ \nu_2 \end{pmatrix}. \quad (13)$$

Quasi-two-neutrino oscillation (Q2N) implies that there is only one relevant mass splitting  $\Delta m_{ij}^2 \rightarrow \Delta m^2$ , that the mixing parameter is real  $\text{Im}(K_{ff'ij}) = 0$ , and that

$$\sum_{i>j} \text{Re}(K_{ff'ij}) = -\sin^2 \theta \cos^2 \theta = -\frac{1}{4} \sin^2 2\theta. \quad (14)$$

The vacuum transition probability in Eq. (12) can be written, for  $\nu_f \neq \nu_{f'}$

$$\begin{aligned} P(\nu_f \rightarrow \nu_f) &= 1 - \sin^2 2\theta \sin^2(1.27\Delta m^2 \frac{L}{E}) \\ P(\nu_f \rightarrow \nu_{f'}) &= \sin^2 2\theta \sin^2(1.27\Delta m^2 \frac{L}{E}), \end{aligned} \quad (15)$$

having restored  $\hbar$  and  $c$  and forced useful units for  $\Delta m^2$  ( $\text{eV}^2$ ),  $L$  (km), and  $E$  (GeV). CP and T invariance are assumed so that  $P(\nu_f \rightarrow \nu_{f'}) = P(\nu_{f'} \rightarrow \nu_f) = P(\bar{\nu}_f \rightarrow \bar{\nu}_{f'})$ .

### 4.1. Three Neutrino Mixing

In other situations, it is appropriate to eschew the Q2N assumption but maintain the assumption of *one mass-scale dominance*,

$$|\Delta m_{12}^2| \ll |\Delta m_{31}^2| \approx |\Delta m_{32}^2|, \quad (16)$$

to obtain a theoretical model of three neutrino mixing [6]. The one mass-scale assumption is appropriate because it has been observed in solar and atmospheric neutrino experiments; it is often written (see Secs. (5.2 & 6.1))

$$\Delta m_{21}^2 \equiv \Delta m_{sol}^2 \sim 10^{-5} \text{eV}^2 \quad (17)$$

$$\Delta m_{32}^2 \equiv \Delta m_{atm}^2 \sim 10^{-3} \text{eV}^2. \quad (18)$$

Any  $3 \times 3$  unitary matrix can be parameterized by three real angles and one imaginary phase. Assuming one mass-scale and neglecting the small CP-violating phase [7], the lepton mixing matrix (analogous to the CKM matrix but called the Maki-Nakagava-Sakata (MNS) matrix) is greatly simplified. The near-degeneracy of  $\nu_1$  and  $\nu_2$  allows for rotating away the mixing angle  $\theta_{12}$  [6]; it is not that  $\theta_{12} \approx 0$ , indeed solar neutrino studies imply  $\theta_{12} \approx 30^\circ$ , but the apparent degeneracy of  $\nu_1$  and  $\nu_2$  makes  $\theta_{12}$  irrelevant. In this way, the  $U_{\text{MNS}}$  matrix (left, with phases neglected) can be parameterized by only two angles as

$$\begin{pmatrix} c_{12} c_{13} & s_{12} c_{13} & s_{13} \\ -s_{12} c_{23} - c_{12} s_{23} s_{13} & c_{12} c_{23} - s_{12} s_{23} s_{13} & c_{13} s_{23} \\ s_{12} s_{23} - c_{12} s_{23} s_{13} & -c_{12} s_{23} - s_{12} c_{23} s_{13} & c_{13} c_{23} \end{pmatrix} \rightarrow \begin{pmatrix} c_{13} & 0 & s_{13} \\ -s_{13} s_{23} & c_{23} & c_{13} s_{23} \\ -s_{13} s_{23} & -s_{23} & c_{13} c_{23} \end{pmatrix} \quad (19)$$

where  $c_{ij} \equiv \cos \theta_{ij}$  and  $s_{ij} \equiv \sin \theta_{ij}$ . Employing the unitarity of  $U_{\text{MNS}}$ ,  $U_{f1}^* U_{f'1} + U_{f2}^* U_{f'2} = -U_{f3}^* U_{f'3}$ , and assuming  $\Delta m_{32}^2 \gg \Delta m_{21}^2$  the transition probabilities from Eq. (12) can be written, to leading order in  $\Delta m_{32}^2$ , as

$$\begin{aligned} P(\nu_e \rightarrow \nu_\mu) &= 4|U_{e3}|^2 |U_{\mu3}|^2 \sin^2 \Delta_{atm} \\ &= \sin^2 \theta_{23} \sin^2 2\theta_{13} \sin^2 \Delta_{atm} \end{aligned} \quad (20)$$

$$\begin{aligned} P(\nu_\mu \rightarrow \nu_\tau) &= 4|U_{\mu3}|^2 |U_{\tau3}|^2 \sin^2 \Delta_{atm} \\ &= \cos^4 \theta_{13} \sin^2 2\theta_{23} \sin^2 \Delta_{atm} \end{aligned} \quad (21)$$

$$\begin{aligned} P(\nu_e \rightarrow \nu_\tau) &= 4|U_{e3}|^2 |U_{\tau3}|^2 \sin^2 \Delta_{atm} \\ &= \cos^2 \theta_{23} \sin^2 2\theta_{13} \sin^2 \Delta_{atm}, \end{aligned} \quad (22)$$

for  $\Delta_{atm} \equiv \Delta m_{32}^2 L/4E$ . This leaves three parameters,  $\theta_{13}$ ,  $\theta_{23}$ , and  $\Delta m_{atm}^2$ , which can be constrained by fitting the probabilities above to data.

In doing so, experimentalists use an initial flavor state with nominal energy  $E$  from one of the four neutrino sources mentioned in Sec. (3) and measure the flux of different final flavor states at a distance  $L$  from the source. It is hoped that the entire parameter space can be redundantly investigated, over-constraining the parameters,  $\Delta m_{ij}^2$  and  $\theta_{ij}$ , and that an oscillation signature as a function of the natural parameter  $L/E$  can be observed.

## 5. THE SOLAR NEUTRINO PROBLEM

The Sun produces energy through the somewhat complicated  $pp$  chain. The “black box” reaction  $4p \rightarrow {}^4\text{He} + 2e^+ + 2\nu_e$  is actually a chain of nuclear fusion, of which the most important link for neutrino studies, is the reaction  ${}^8\text{B} \rightarrow {}^8\text{Be} + e^+ + \nu_e$ . According to the standard solar model (SSM), the  $\nu_e$  from this interaction have an approximate energy ( $E_\nu$ ) of 15 MeV and flux of  $5 \times 10^6 \text{ cm}^{-2} \text{ s}^{-1}$ . Except the reaction  ${}^3\text{He} + p \rightarrow {}^4\text{He} + e^+ + \nu_e$  which has a flux one thousand times smaller than the  ${}^8\text{B}$  decay, all other neutrino source reactions in the Sun have  $E_\nu < 2 \text{ MeV}$ , less than the trigger energy of typical detectors.

The first solar neutrino data was published by R. Davis in 1968 [8]. His tank of 390,000 liters of  $\text{C}_2\text{Cl}_4$  sat 1480 meters below the surface in the Homestake Mine in Lead, South Dakota. Primarily detecting neutrinos from solar  ${}^8\text{B}$  decays through the interaction  $\nu_e + {}^{37}\text{Cl} \rightarrow e^- + {}^{37}\text{Ar}$ , Davis measured a capture rate  $2.56 \pm 0.16 \pm 0.16 \times 10^{-36}$  captures/atom/s, about one third that predicted by the SSM. A discrepancy was apparent, but the cause: either Davis’s experiment, the SSM, or neutrino physics, was undetermined.

### 5.1. Super-Kamiokande and SNO

Located in the Kamioka mine in Japan, SuperK uses an array of photomultiplier (PM) tubes to detect the Cherenkov light produced by electrons in water which have scattered with  $\nu_e$ ,  $\nu_\mu$ , and  $\nu_\tau$ . The directionality of the Cherenkov cones allowed SuperK to measure a zenith angle and confirm that the neutrinos are indeed of solar origin. Elastic scattering  $e^- - \nu_{\mu,\tau}$  only occurs through the neutral current and is suppressed relative to  $e^- - \nu_e$  scattering. With a threshold on the order of 5 MeV, SuperK measures the  ${}^8\text{B}$   $\nu_e$  flux to be

$$\Phi({}^8\text{B}) = 2.35 \pm 0.02 \pm 0.08 \times 10^6 \text{ cm}^{-2} \text{ s}^{-1}, \quad (23)$$

about half that of the SSM prediction [5]. The high statistics of SuperK greatly strengthened the veracity of Davis’s measurement, but did not resolve whether the deficit was due to a poor SSM or a poor understanding of neutrino physics.

The Sudbury Neutrino Observatory (SNO) in Ontario, Canada also employs a Cherenkov light detector. However, the use of heavy water ( $\text{D}_2\text{O}$ ) allows the study of deuterium disintegration which yields more insight into the solar neutrino anomaly. Deuteron breakup through the charged weak current (CC),  $\nu_e + d \rightarrow e^- + p + p$ , is sensitive only to  $\nu_e$  at the energy of

solar neutrinos. Elastic scattering (ES), as used in SuperK, is sensitive to all flavors, but is not sensitive to the absolute flux. The neutral weak current (NC),  $\nu + d \rightarrow \nu + p + n$ , being independent of flavor, gives the total  $\nu$  flux. In 2002, SNO published a solar  $\nu_\mu + \nu_\tau$  flux  $5.3\sigma$  from zero [9]

$$\phi_{\mu\tau} = 3.41_{-0.45}^{+0.45} (\text{stat})_{-0.45}^{+0.48} (\text{syst}) \times 10^6 \text{ cm}^{-2} \text{ s}^{-1}, \quad (24)$$

and a total neutrino flux

$$\phi_{\text{NC}}^{\text{SNO}} = 5.09_{-0.43}^{+0.44} (\text{stat})_{-0.43}^{+0.46} (\text{syst}) \times 10^6 \text{ cm}^{-2} \text{ s}^{-1}, \quad (25)$$

in excellent agreement with the  $\phi_{\text{SSM}} = 5.05_{-0.81}^{+1.01} \times 10^6 \text{ cm}^{-2} \text{ s}^{-1}$ , thereby confirming neutrino mixing as the cause of the solar neutrino problem.

## 5.2. Theory of Solar Neutrino Oscillation: Matter Matters

Atmospheric and reactor neutrino studies (see Secs. (7 & 6.2)) have placed an upper limit of  $\theta_{13} < 9^\circ$  that is consistent with  $\theta_{13} = 0^\circ$ . Because  $\theta_{13}$  is small, one can see from the left side of Eq. (19) that  $\nu_3$  plays little role in the mixing of solar  $\nu_e$ . This mixing can then be viewed as Q2N mixing between  $\nu_e$  and a state  $\nu_x$  that is a linear combination of  $\nu_\mu$  and  $\nu_\tau$ :

$$\begin{pmatrix} \nu_e \\ \nu_x \end{pmatrix} = \begin{pmatrix} \cos \theta_{12} & \sin \theta_{12} \\ -\sin \theta_{12} & \cos \theta_{12} \end{pmatrix} \begin{pmatrix} \nu_1 \\ \nu_2 \end{pmatrix}. \quad (26)$$

A complete rendering of the theory of neutrino flavor change in matter, the Mikheyev-Smirnov-Wolfenstein (MSW) effect, is beyond the scope of this paper, but a qualitative summary is useful. Electron neutrinos created in center of the sun travel  $7 \times 10^8$  meters through matter with a density as large as  $150 \text{ g/cm}^3$ , and the effects of scattering with electrons greatly influences their evolution. The MSW theory describes neutrino propagation through matter with a ‘‘Schrodinger-like equation [4].’’ It neglects NC interaction energy, but includes CC interaction energy,  $\Delta m_{12}^2$ , and  $\theta_{12}$  in the effective Hamiltonian governing the propagation.

The theory shows that for certain  $\Delta m_{12}^2$  the mass eigenstates are simultaneously eigenstates of the effective Hamiltonian. A  $\nu_e$  created in the sun propagates as the heavier of the two simultaneous eigenstates which is defined to be  $\nu_2$  [4]. When it leaves the sun it is in

a stationary state and therefore propagates through the vacuum without oscillation. Equation (26) shows that  $\nu_2$  can be written as a linear combination  $\nu_2 = \sin \theta_{12} \nu_e + \cos \theta_{12} \nu_x$ , making the probability of detecting a solar neutrino as  $\nu_e$  at *any*  $L$

$$P(\nu_{sol} \rightarrow \nu_e) = \sin^2 \theta_{12}. \quad (27)$$

Best-fits of the SuperK and SNO data to the MSW theory favor two solutions, the Large Mixing Angle (LMA) and Long Oscillation Wavelength (LOW) solutions [4]

$$\text{LMA: } \Delta m_{12}^2 \approx 7 \times 10^{-5} \text{eV}^2 \quad \text{and} \quad \theta_{12} = 32.5^\circ \quad (28)$$

$$\text{LOW: } \Delta m_{12}^2 \approx 1 \times 10^{-7} \text{eV}^2 \quad \text{and} \quad \theta_{12} = 39.3^\circ \quad (29)$$

A Small Mixing Angle solution was originally favored as corresponding with the quark sector, but has been excluded by SNO to  $3.6\sigma$  [4].

### 5.3. KamLAND

More information was needed to rule out either the LMA or LOW solution for solar neutrino oscillation. The KamLAND long baseline (LBL) reactor experiment attempted to accomplish this goal by searching for  $\bar{\nu}_e$  disappearance. Also installed in the Kamioka mine in Japan, the detector sits within 140 to 210 km of sixteen commercial nuclear reactors. A baseline of  $10^5$  meters coupled with reactor neutrino energies of 10 MeV gives KamLAND sensitivity to  $\Delta m^2$  in the same region as the LMA solution, see Table (I).

The detector is a stainless steel vessel containing 1000 tons of mineral oil liquid scintillator. The neutrinos are detected through the interaction  $\bar{\nu}_e + p \rightarrow n + e^+$ ; the 1280 PM tubes surrounding the scintillator detect the delayed coincidence of prompt photons from positron annihilation and delayed photons from neutron capture.

KamLAND found evidence of oscillation by measuring the ratio of observed events less expected background to the number expected without oscillation [10]

$$\frac{N_{\text{obs}} - N_{\text{BG}}}{N_{\text{NoOsc}}} = 0.611 \pm 0.085 \text{ (stat)} \pm 0.041 \text{ (syst)}. \quad (30)$$

Figure (2) suggests that other reactor experiments did not observe oscillation because they were measuring at too small an  $L/E$ . Figure (2) also shows that KamLAND's results not only were consistent with the LMA solution, but also ruled out the LOW and other solutions with  $\Delta m^2 < 10^{-5}$ .

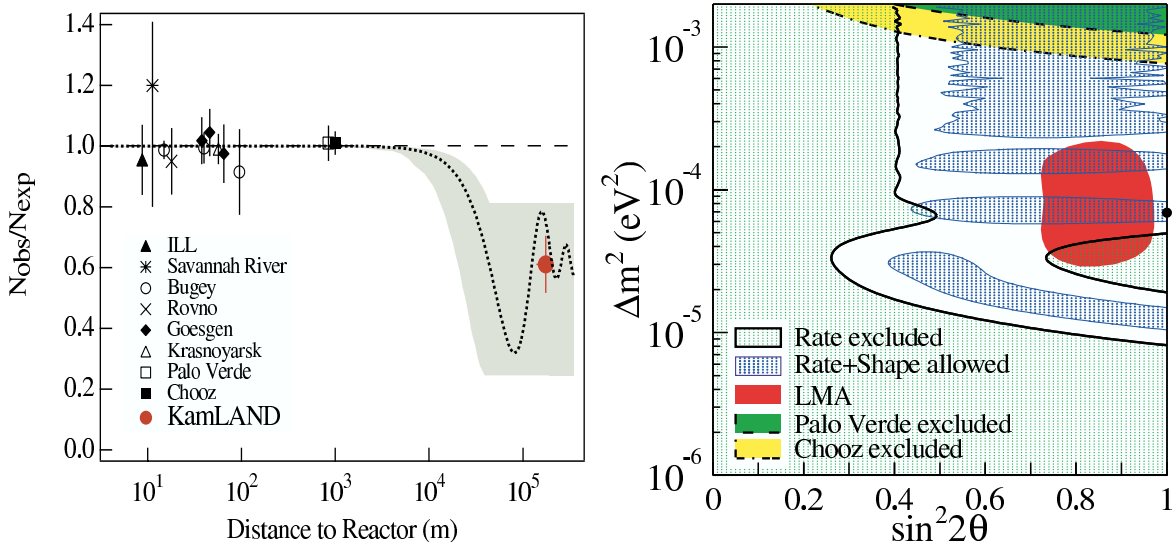


FIG. 2: The ratio of observed to expected (without oscillation)  $\bar{\nu}_e$  flux from nine reactor experiments (*left*). KamLAND’s result is plotted at a “flux-weighted average distance of 180 km,” the shaded region corresponds with  $\bar{\nu}_e$  flux predicted at 95% CL by the LMA solution (see Sec. (5.2)), and the dotted curve is the LMA predicted flux for  $\sin^2 2\theta = 0.833$  and  $\Delta m^2 = 5.5 \times 10^{-5} \text{ eV}^2$  [10]. On the *right* is KamLAND’s allowed parameter space in *blue* and the LMA prediction in *red* at 95% CL. The excluded region of CHOOZ is in *yellow*. The black dot is the best-fit value for KamLAND data:  $\sin^2 2\theta = 1$  and  $\Delta m^2 = 6.9 \times 10^{-5} \text{ eV}^2$  [10].

## 6. THE ATMOSPHERIC NEUTRINO PROBLEM

Atmospheric neutrinos result from the interaction of hadronic cosmic rays with the atmosphere that create showers of hadronic particles. The primary interactions yielding neutrinos are the decay of charged pions and the secondary decay of daughter muons

$$\pi^+ \rightarrow \mu^+ \nu_\mu \quad \mu^+ \rightarrow e^+ \nu_e \bar{\nu}_\mu \quad (+ \text{c.c.'s}). \quad (31)$$

Leptonic and semi-leptonic kaon decays also contribute to the neutrino flux, and are the primary  $\nu_e$  source at higher energies where muons reach the earth before decaying. While absolute flux predictions are notoriously unreliable, the ratio of muon to electron neutrinos can be calculated to within about 5% [11]. Typically, the ratio

$$R = \frac{[N(\mu\text{-like})/N(e\text{-like})]_{\text{observed}}}{[N(\mu\text{-like})/N(e\text{-like})]_{\text{expected}}} \quad (32)$$

is calculated, and deviation from  $R = 1$  implies oscillation. This is neither an appearance nor disappearance measurement, and  $R \neq 1$  can imply several net scenarios:  $\nu_\mu \rightarrow \nu_e$ ,  $\nu_\mu \rightarrow \nu_\tau$ ,

$\nu_e \rightarrow \nu_x$ , etc.; i.e. oscillations can be detected, but the specific underlying mode and information about parameters are hidden.

### 6.1. Super-Kamiokande - Atmospheric Mode

The Super-Kamiokande detector is instrumental in the unraveling of the atmospheric neutrino puzzle. The 22 kiloton fiducial volume of SuperK gave an unprecedented  $E_\nu$  sensitivity from  $\sim 100$  MeV - 1 TeV. Flight distances ranging from 10 km to 12000 km gave  $\Delta m^2$  sensitivity between  $10^{-4}$  and  $10^{-1}$  eV<sup>2</sup>. The Cherenkov light from muons and electrons created in CC interactions of  $\nu_{\mu,e}$  with neutrons in water was detected with PM tubes; muon- and electron-like events were distinguished by the relative sharpness of the Cherenkov rings in muon-like events. The collaboration confirmed oscillation with a measurement

$$R = 0.675_{-0.032}^{+0.034} (\text{stat})_{-0.08}^{+0.08} (\text{syst}). \quad (33)$$

A more illuminating measurement was the difference over sum ratio of up-going to down-going neutrinos for *fully contained* (FC) neutrino events. FC events, comprising two thirds of the data-set, are those for which the initial neutrino interaction and the track of the resulting muon or electron are contained within the detector. The charged particle's energy, direction, and flavor are well determined for these events.

The SuperK collaboration observed a deficit of up-going  $\nu_\mu$  at  $\mu$ -momentum greater than 1 GeV and a  $\nu_e$  pattern consistent with no oscillation, see Fig. (3). The collaboration concluded that the atmospheric neutrino anomaly is due to disappearing muons ( $\nu_\mu \rightarrow \nu_\tau$ ), that there is little  $\nu_\mu$ - $\nu_e$  coupling at this range of  $\Delta m^2$ , and that the  $\nu_\mu$  mixing must be nearly maximal. In 2004, SuperK published the first sinusoidal oscillation signature, also Fig. (3).

Using the Q2N assumption, which is appropriate since  $\nu_\mu \rightarrow \nu_\tau$  is the only oscillation mode, the best-fit values for the parameters in Eq. (15) are [12]

$$\Delta m_{atm}^2 = 2.4 \times 10^{-3} \text{ eV}^2 \quad \text{and} \quad \sin^2 2\theta_{atm} = 1.02. \quad (34)$$

The value for  $\sin^2 2\theta$  is usually restricted to the physical region and set to one.

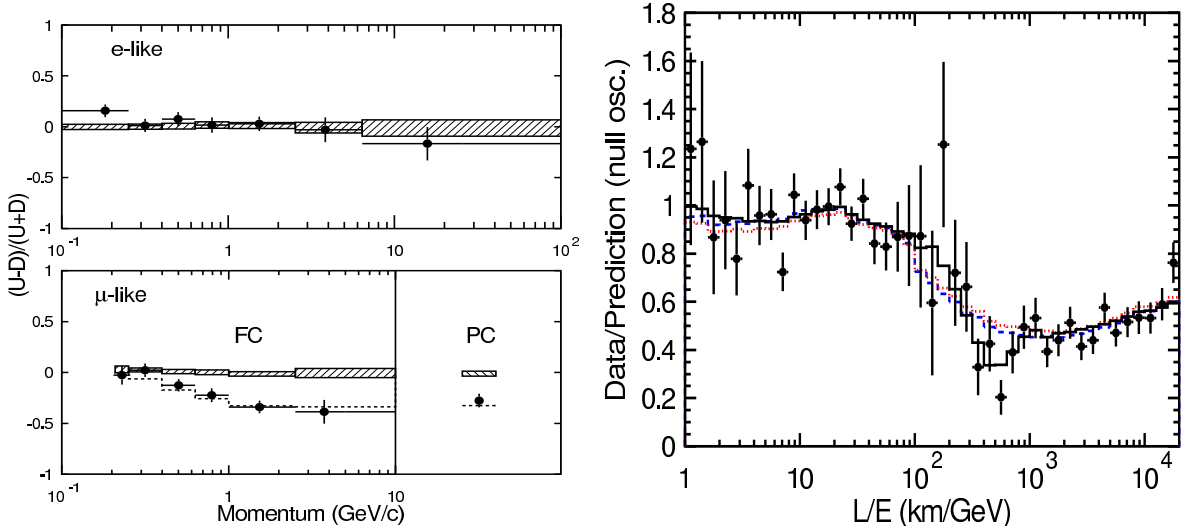


FIG. 3: The assymetry between up- and down-going events as a function of  $\mu, e$  momentum for muon and electron events from the FC event data-set of SuperK (*left*). The hatched region is the assymetry expected with no oscillations; the dashed line is that expected for  $\nu_\mu \rightarrow \nu_\tau$  oscillation with  $\Delta m^2 = 2.2 \times 10^{-3} \text{eV}^2$  and  $\sin^2 2\theta = 1$  [13]. The oscillation pattern in the ratio of data to non-oscillation MC as a function of the natural parameters  $L/E$  (*right*); the solid line is the expectation for  $\nu_\mu \rightarrow \nu_\tau$  oscillation [12].

## 6.2. The CHOOZ Experiment

The current understanding of atmospheric neutrino data does not involve significant  $\nu_\mu \rightarrow \nu_e$  oscillation. This claim is motivated by the SuperK atmospheric data, see Fig. (3), but independent confirmation is reassuring. The CHOOZ detector, sitting a little over 1 km from two nuclear reactors in France, was sensitive to  $\Delta m^2$  down to  $10^{-3} \text{eV}^2$ , *completely* covering the region favored by the SuperK atmospheric data. As a disappearance experiment, CHOOZ looked for the oscillation  $\bar{\nu}_e \rightarrow \bar{\nu}_x$  in the deficit of expected  $\bar{\nu}_e$ . From Eqs. (20 & 22) one can see that the probability of detecting an initial  $\bar{\nu}_e$  as a  $\bar{\nu}_e$  is

$$P(\bar{\nu}_e \rightarrow \bar{\nu}_e) = 1 - P(\bar{\nu}_e \rightarrow \bar{\nu}_\mu) - P(\bar{\nu}_e \rightarrow \bar{\nu}_\tau) \quad (35)$$

$$= 1 - \sin^2 \theta_{23} \sin^2 2\theta_{13} \sin^2 \Delta_{atm} - \cos^2 \theta_{23} \sin^2 2\theta_{13} \sin^2 \Delta_{atm} \quad (36)$$

$$= 1 - \sin^2 2\theta_{13} \sin^2 \Delta_{atm}. \quad (37)$$

The collaboration measured the ratio of observed events to events expected without oscillation to be  $R = 1.01 \pm 2.8\% \pm 2.7\%$  and placed an upper limit of  $\sin^2 2\theta_{13} < 0.1$  (90% CL)

at  $\Delta m^2 \approx 3 \times 10^{-3} \text{ eV}^2$  [14].

## 7. CONSTRAINING THE PARAMETERS - SUMMARY

The ultimate goal is to make consistent, independent measurements of the six (assuming three flavors and no CP violation) parameters describing neutrino oscillation. Five parameters have been measured or constrained as described in Secs. (6.1, 5.2, & 6.2):  $\Delta m_{sol}^2$ ,  $\Delta m_{atm}^2$ ,  $\theta_{sol}$ ,  $\theta_{atm}$ , and  $\theta_{13}$ . In Sec. (5.2), the measured solar mass-splitting and angle were related to the oscillation parameters as  $\Delta m_{sol}^2 = \Delta m_{21}^2$  and  $\theta_{sol} = \theta_{12}$ . In Sec. (6.2), an upper limit was placed on  $\theta_{13}$ , but it still remains to relate the remaining parameters  $\Delta m_{ij}^2$  and  $\theta_{ij}$  to  $\Delta m_{atm}^2$  and  $\theta_{atm}$ .

Considering that  $\Delta m_{sol}^2 \ll \Delta m_{atm}^2$  and  $\Delta m_{12}^2 + \Delta m_{23}^2 + \Delta m_{31}^2 = 0$ , one can define  $\Delta m_{21}^2$  and  $\Delta m_{32}^2$  as done in Eqs. (17 & 18), and one finds that  $\Delta m_{31}^2 \approx \Delta m_{32}^2$ . The determination that  $\Delta m_{sol}^2 \ll \Delta m_{atm}^2$  also allows for the three neutrino mixing assumption made in Sec. (4.1) and the derivation of Eqs. (20-22) which are indispensable for understanding  $\Delta m_{atm}^2$  and  $\theta_{atm}$ . By comparing Eqs. (21 & 15) for small  $\theta_{13}$  (as confirmed by CHOOZ), SuperK's best-fit values from Eq. (34) can be identified as  $\theta_{atm} = \theta_{32}$  and  $\Delta m_{atm}^2 = \Delta m_{32}^2$ . As a check one can consider Eqs. (20 & 21): taking  $\theta_{23} = \theta_{atm}$  and  $\theta_{13} = \text{small}$  leads to a minimization of  $P(\nu_e \rightarrow \nu_\mu)$  and a maximization of  $P(\nu_\mu \rightarrow \nu_\tau)$ , as expected. The current best-fit values and limits for the six parameters:

$$\begin{aligned} \Delta m_{21}^2 &= 7.1 \times 10^{-5} \text{ eV}^2 & \theta_{12} &= 32.5^\circ \\ \Delta m_{32}^2 &= 2.4 \times 10^{-3} \text{ eV}^2 & \theta_{23} &= 45^\circ \\ \Delta m_{31}^2 &= 2.4 \times 10^{-3} \text{ eV}^2 & \theta_{13} &< 9.2^\circ \quad (90\% \text{ CL}). \end{aligned}$$

## 8. OUTSTANDING ISSUES: THE LSND PROBLEM

The LSND experiment at Los Alamos National Laboratory primarily looked for  $\bar{\nu}_\mu \rightarrow \bar{\nu}_e$  oscillation using the decay at rest of  $\mu^+$  through the interaction  $\bar{\nu}_e + p \rightarrow e^+ + n$ . Primary backgrounds from  $\mu^-$  and  $\pi^-$  decay were suppressed by capture of those particles in the nuclei of the intermediate shielding and beam dump. After background subtraction, LSND measured an excess of  $87.9 \pm 22.4 \pm 6.0 \bar{\nu}_e$  events, see Fig. (4), which corresponds with an

oscillation probability [15]

$$P(\bar{\nu}_\mu \rightarrow \bar{\nu}_e) = (0.264 \pm 0.067 \pm 0.045)\%. \quad (38)$$

The collaboration found best-fit values of

$$\Delta m_{LSND}^2 = 1.2 \text{ eV}^2 \quad \sin^2 2\theta_{LSND} = 0.003. \quad (39)$$

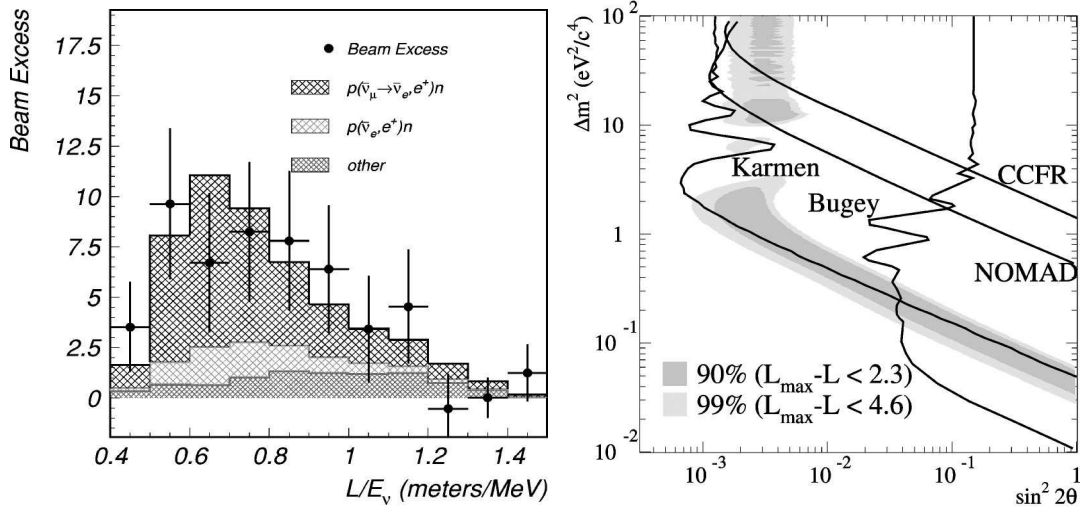


FIG. 4: The distribution of  $\bar{\nu}_e$  events as a function of  $L/E$  (left). The data points are plotted with the background expectation (light hatched) and the expected flux for  $\bar{\nu}_\mu \rightarrow \bar{\nu}_e$  oscillation (dark hatched). The  $\Delta m^2$ - $\sin^2 2\theta$  parameter fit at 90% and 99% C.L. for the entire data-set (right). Limits from other experiments are shown at 90% C.L; the Karmen experiment which was very similar to LSND excludes most of the LSND allowed region [15].

While there are no clear flaws in the analysis, the LSND observation is not as compelling as the solar and atmospheric measurements, because it is unexpected theoretically and the statistical significance of the measurement is not high, about  $4\sigma$ . The problem with the LSND measurement is that  $\Delta m_{LSND}^2 \sim 1 \text{ eV}^2$  is incompatible with previous measurements,  $\Delta m_{sol}^2 \sim 10^{-5} \text{ eV}^2$  and  $\Delta m_{atm}^2 \sim 10^{-3} \text{ eV}^2$ , and the requirement  $\Delta m_{12}^2 + \Delta m_{23}^2 + \Delta m_{31}^2 = 0$  for *three* mass eigenstates.

An immediate explanation is that there are *four* mass and flavor eigenstates. The fourth flavor state, currently unobserved, is called a *sterile* neutrino because, lacking a charged lepton partner, it cannot couple with the  $W$  boson, and as seen in Sec. (1), the  $Z^0$  width indicates that the  $Z^0$  couples to light neutrinos of only three flavors. This hypothesis is not

absurd: important experiments, such as SuperK and its observation of  $\nu_\mu \rightarrow \nu_x$ , measure only  $\nu_\mu$  disappearance where it is *assumed* that  $\nu_x = \nu_\tau$ , but it is possible that  $\nu_x$  is a sterile neutrino.

For this reason, it is necessary that the angles of the MNS matrix, especially  $\theta_{13}$  for which there are only upper limits, be measured more precisely. When this is accomplished, a total probability  $P(\nu_\alpha \rightarrow \nu_e) + P(\nu_\alpha \rightarrow \nu_\mu) + P(\nu_\alpha \rightarrow \nu_\tau) \neq 1$  would guarantee the existence of sterile neutrinos. Additionally, *appearance* experiments directly measuring  $P(\nu_\alpha \rightarrow \nu_\tau)$  are necessary as a check. The first step is to confirm the LSND result with higher statistics and different systematics: The MiniBooNE experiment at Fermilab began taking data in 2002 to probe the  $\Delta m_{LSND}^2$  region, see Table(I); they expect to publish a result in the fall of 2005 [16].

## 9. CONCLUSION AND FUTURE EXPERIMENTS

The observation of neutrino mixing implies a non-vanishing neutrino mass. Lepton and quark mixing are each described by a unitary matrix relating their respective mass and flavor bases, lepton mixing is characterized by two large mixing angles where quark mixing is minimal. When quarks are produced as weak eigenstates, they immediately collapse into stationary states through electromagnetic and strong interactions. Neutrinos, interacting only weakly, are not forced to collapse and can oscillate over macroscopic distances. These oscillations are characterized by the angles of the MNS matrix and the differences of the squared masses of the stationary states.

A number of experiments have measured these parameters: SNO and SuperK in the solar sector, SuperK in the atmospheric sector, and KamLAND and CHOOZ at nuclear reactors. The imprecision of the existing measurements and the inconsistent LSND observation demand novel experiments to measure these parameters with better statistics and different systematic errors. MiniBooNE is a strong start for testing the LSND measurement. A promising group of new experiments are the LBL accelerator experiments such as K2K in Japan, which after one year of data-taking has best-fit values,  $\Delta m^2 = 2.8 \times 10^{-3} \text{ eV}^2$  and  $\sin^2 2\theta = 1.03$  [17], in excellent agreement with previous measurements. The *high-energy*, LBL experiments such as MINOS in the United States, CERN-Gran Sasso in Europe, and an upgraded K2K are poised to observe  $\nu_\mu \rightarrow \nu_\tau$  appearance with energies above the  $\tau$

threshold energy of 3.5 GeV.

The most exciting aspect of physics is that things are seldom what they seem; this is certainly true of neutrino physics.

- 
- [1] K. Winter, ed., *Neutrino Physics* (Cambridge University Press, 2000).
  - [2] F. Reines and C. Cowan, *Phys. Rev.* **92**, 830 (1953).
  - [3] R. Davis, *Phys. Rev.* **97**, 766 (1955).
  - [4] S. Eidelman et al., *Phys. Lett.* **B592**, 1 (2004).
  - [5] K. Zuber, *Neutrino Physics* (Institute of Physics Publishing, 2004).
  - [6] G. Fogli, E. Lisi, and G. Scioscia, *Phys. Rev.* **D52**, 5334 (1995).
  - [7] G. Fogli, E. Lisi, and D. Montanino, *Phys. Rev.* **D49**, 3626 (1994).
  - [8] R. Davis, D. Harmer, and K. Hoffman, *Phys. Rev. Lett.* **20**, 1205 (1968).
  - [9] Q. Ahmad et al., *Phys. Rev. Lett.* **89**, 011301 (2002).
  - [10] K. Eguchi et al., *Phys. Rev. Lett.* **90**, 021802 (2003).
  - [11] D. O. Caldwell, ed., *Current Aspects of Neutrino Physics* (Springer, 2001).
  - [12] Y. Ashie et al., *Phys. Rev. Lett.* **93**, 101801 (2004).
  - [13] Y. Fukuda et al., *Phys. Rev. Lett.* **81**, 1562 (1998).
  - [14] M. Apollonio et al., *Phys. Lett.* **B466**, 415 (1999).
  - [15] A. Aguilar et al., *Phys. Rev.* **D64**, 112007 (2001).
  - [16] E. D. Zimmerman, *Private communication* (2005).
  - [17] M. Ahn et al., *Phys. Rev. Lett.* **90**, 041801 (2003).